Rayleigh statistics of waves in integrable nonlinear systems

**V.E. Zakharov in collaboration with D.S. Agafontsev (Moscow, Russia)
and A.A. Gelash (Novosibirsk, Russia)**

We will discuss the focusing Nonlinear Schrodinger equation (NLSE) with the following Initial Conditions (IC):

I. Condensate IC

II. Cnoidal wave IC

III. Soliton gas IC

Statistics of waves for linear systems.

Let us suppose, that wave field **ψ** is a random superposition of a multitude of uncorrelated linear waves,

$$\psi(x) = \sum_k |\psi_k| \, e^{i(kx+\phi_k)}.$$

If phases $\boldsymbol{\varphi_k}$ are random and uncorrelated, the number of waves **{k}** is large, and amplitudes $\boldsymbol{\psi_k}$ fall under the conditions of central limit theorem, then real **Re ψ** and imaginary **Im ψ** parts are Gaussian-distributed, and the probability density function (PDF) for wave amplitude is Rayleigh distribution,

$$\mathrm{P}_R(|\psi|) = \frac{2|\psi|}{\sigma^2} e^{-|\psi|^2/\sigma^2}.$$

Here $\boldsymbol{\sigma^2 = \langle|\psi|^2\rangle}$, and the PDF is normalized as

$$\int \mathrm{P}\,(|\psi|)\, d\,|\psi| = 1.$$

For convenience, we study PDFs for relative intensity $\boldsymbol{I = |\psi|^2 / \sigma^2}$, and Rayleigh PDF in this case takes a simple form:

$$\mathrm{P}_R(I) = e^{-I}.$$

For nonlinear systems (1) the spectrum $\boldsymbol{\psi_k}$ changes with time and may have singularities and (2) the phases $\boldsymbol{\varphi_k}$ are correlated. This means that evolution may lead to non-Rayleigh PDF and enhanced appearance of rogue waves.

Numerical experiments with NLSE – condensate IC.

We study statistics of waves for the Nonlinear Schrodinger equation (NLSE),

$$i\psi_t + \psi_{xx} + |\psi|^2 \psi = 0,$$

for the problem of modulational instability (MI) of the condensate

$$\psi|_{t=0} = 1 + \mathrm{T}(x), \quad |\mathrm{T}(x)| << 1.$$

Initial perturbation **τ(x)** is statistically homogeneous in space (not localized). We use Runge-Kutta 4th-order method on adaptive grid, which conserves very well the first 12 integrals of motion (with error smaller than 10^{-6}). To calculate statistics, we use ensembles of 1000 initial distributions. Note that in our case $\boldsymbol{\sigma^2 = \langle|\psi|^2\rangle = 1}$, so that the relative intensity is equal to the square amplitude, $\boldsymbol{I = |\psi|^2}$.

We observe that the system asymptotically approaches to its stationary state in oscillatory way (left – kinetic and potential energies, right – moments of 1st, 3rd and 4th orders):

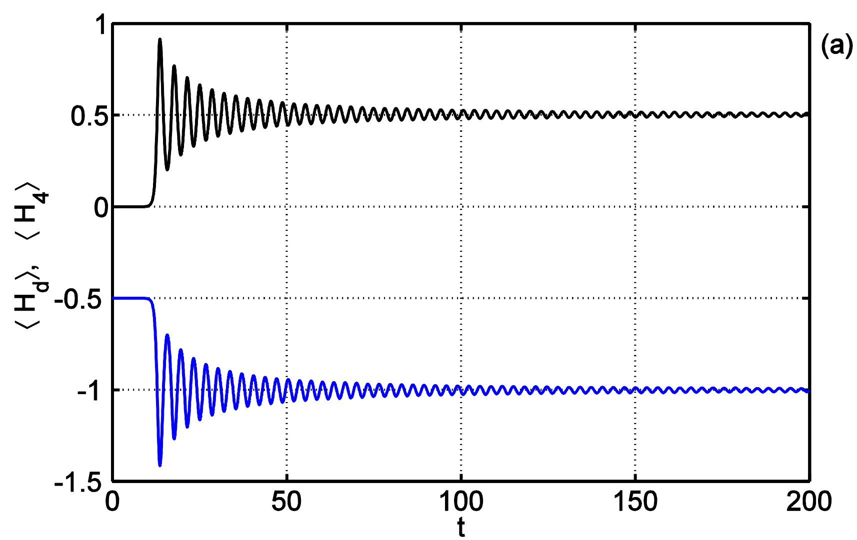

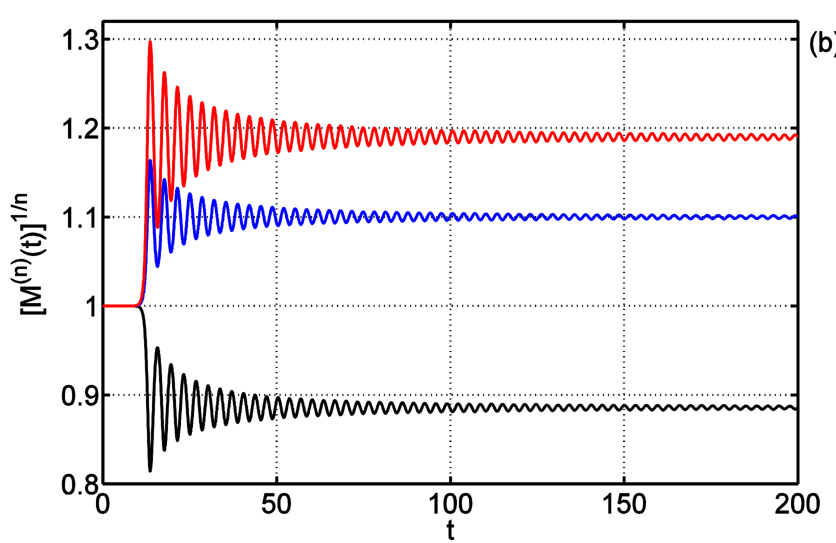

Numerical experiments with NLSE – condensate IC.

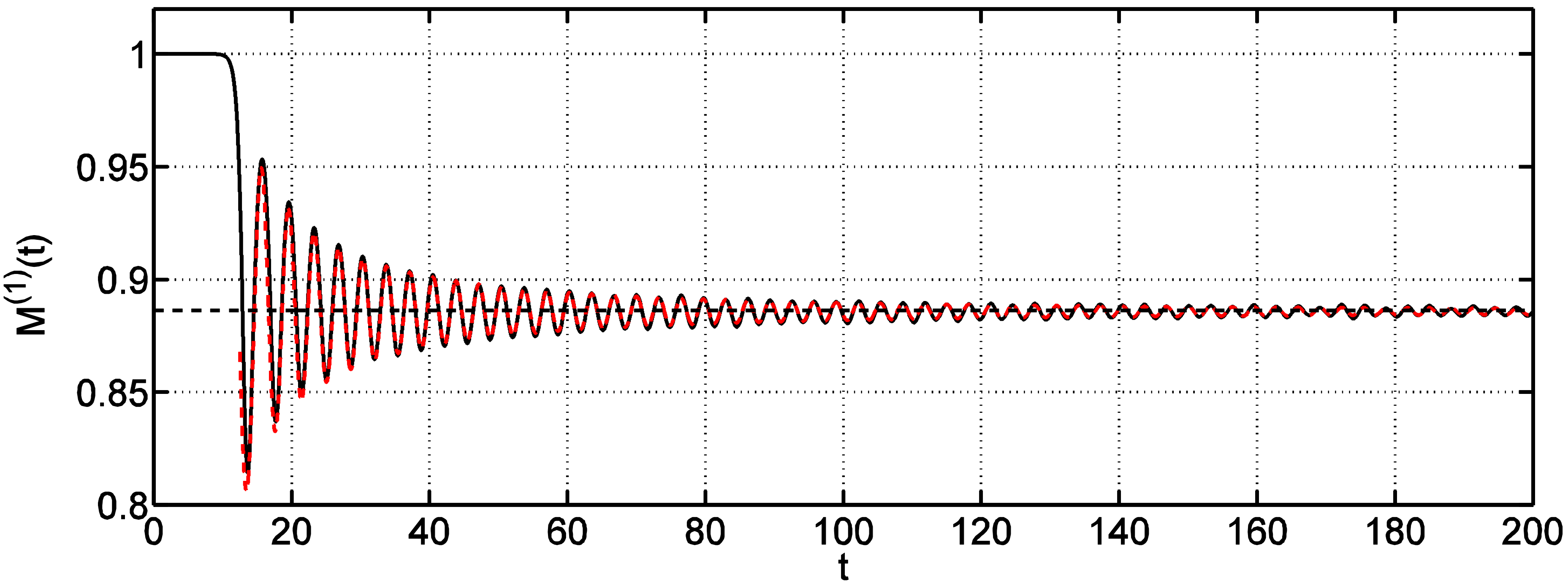

Oscillations of the moments are very well approximated by the model function,

$$M^{(n)}(t) \equiv \langle |\psi|^n \rangle \approx M_A^{(n)} + \frac{p}{t^{3/2}} \sin(\Phi(t)), \quad \Phi(t) = st + \phi_{nl}(t) + \Phi_0, \quad \phi_{nl}(t) = \frac{q}{t^{1/2}}.$$

where $\mathbf{M_A^{(n)}}$ is asymptotic (Rayleigh) value, **s ≈ 2** is the frequency (equal to the double maximum growth rate of the MI), and ϕ_{nl} is the nonlinear phase shift. The first 4 extremums of the oscillations are: t = 13.7 (minimum), t = 15.8 (maximum), t = 17.7 (minimum), t = 19.6 (maximum).

Numerical experiments with NLSE – condensate IC.

In the asymptotic state the PDF and the moments are Rayleigh ones (black – experimental values, red – Rayleigh ones),

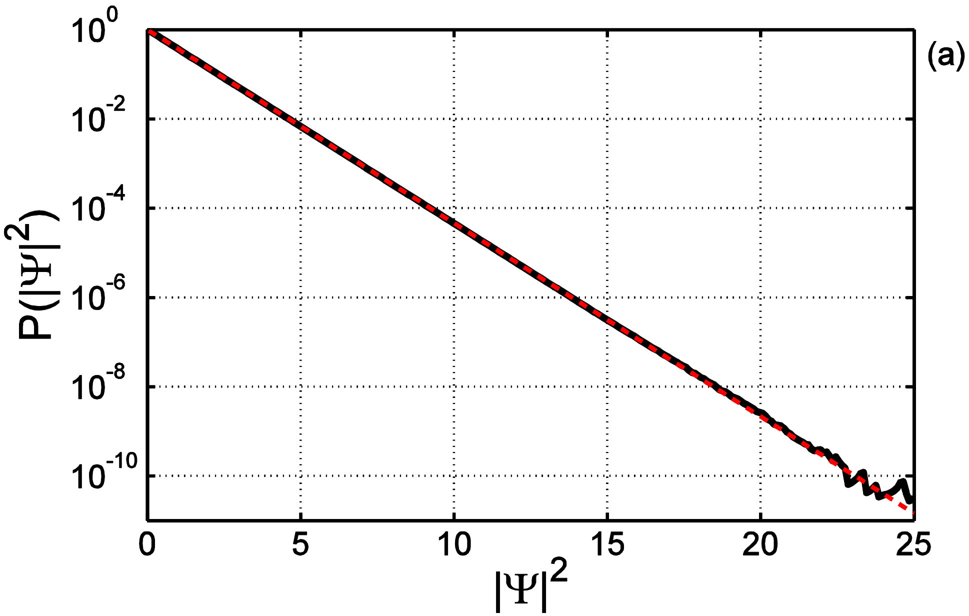

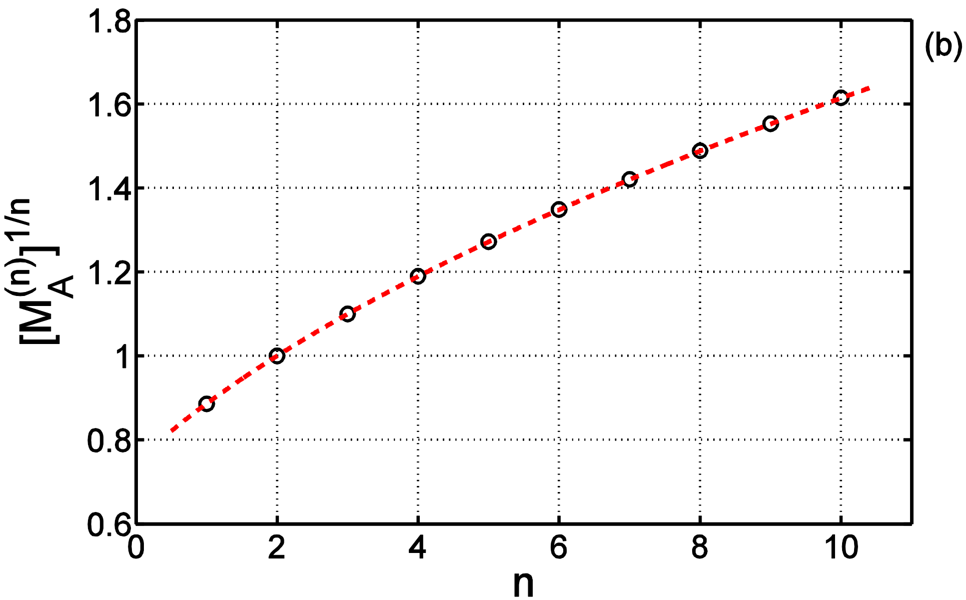

$$P(|\psi|^2) = e^{-|\psi|^2} \qquad M^{(n)} = \Gamma\left(n/2+1\right)$$

while the potential energy, **$\langle H_4 \rangle$ = -1**, is two times larger than the kinetic one, **$\langle H_d \rangle$ = 0.5**.

Numerical experiments with NLSE – condensate IC.

While the system asymptotically approaches to its stationary state, the PDF of wave intensity oscillates around Rayleigh PDF (thick red line),

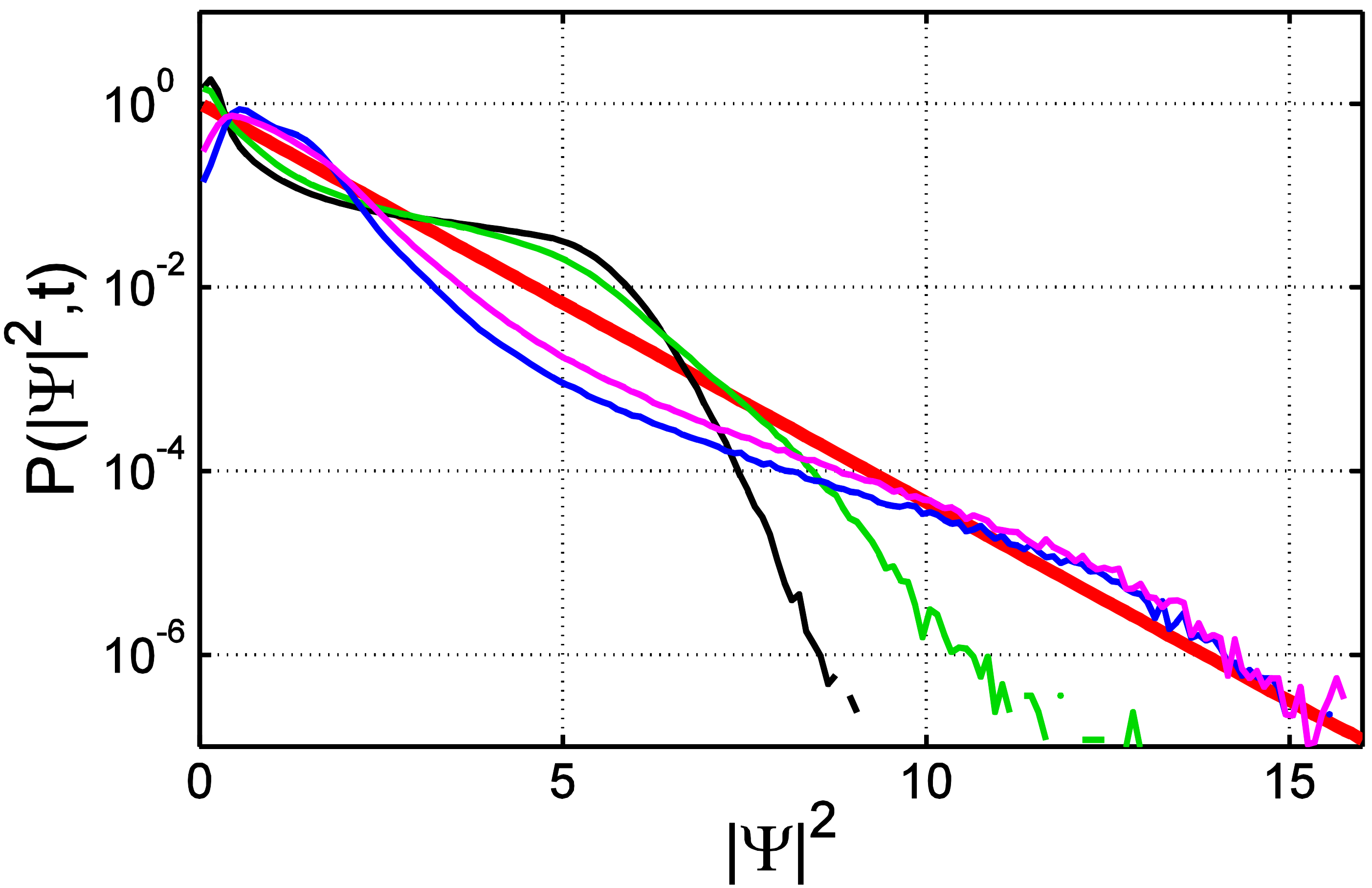

After the system reaches its nonlinear stage of the modulational instability, and at times **t** when the absolute value of the potential energy **$|H_4(t)|$** takes its local maximums, the probability of rogue waves **$|\psi|^2>8$** appearance is about 2-3 times higher than in case of Rayleigh PDF.

Numerical experiments with NLSE – cnoidal wave IC.

We observe the similar results for the modulational instability of cnoidal waves,

$$i\psi_t + \psi_{xx} + |\psi|^2 \psi = 0,$$

$$\psi|_{t=0} = \sqrt{2}\,\nu\ \mathrm{dn}(\nu x; s^2) + \mathrm{T}(x), \quad |\mathrm{T}(x)| << 1,$$

where **dn(x)** is the Jacobi elliptic function, while **v** and **s** are its parameters. Cnoidal waves are the exact periodic solutions of the NLS equation, which can be represented as a lattice of solitons (in the figure below: black – cnoidal wave, red – NLS soliton).

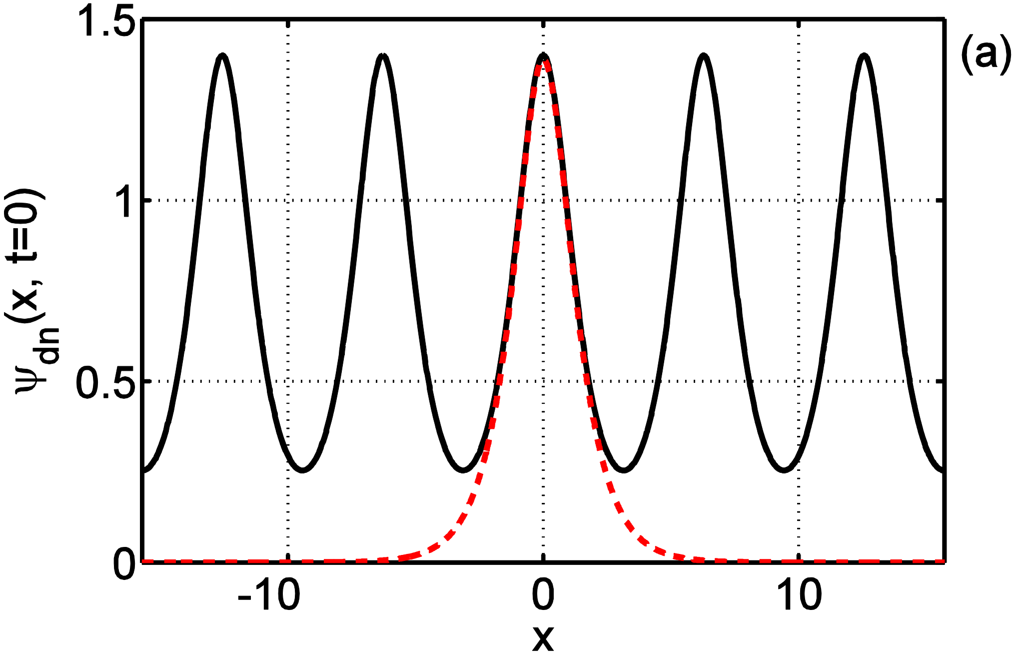

Modulational instability of these lattices leads to integrable turbulence.

As for the condensate initial conditions, the system asymptotically approaches its stationary state in oscillatory way.

Numerical experiments with NLSE – cnoidal wave IC.

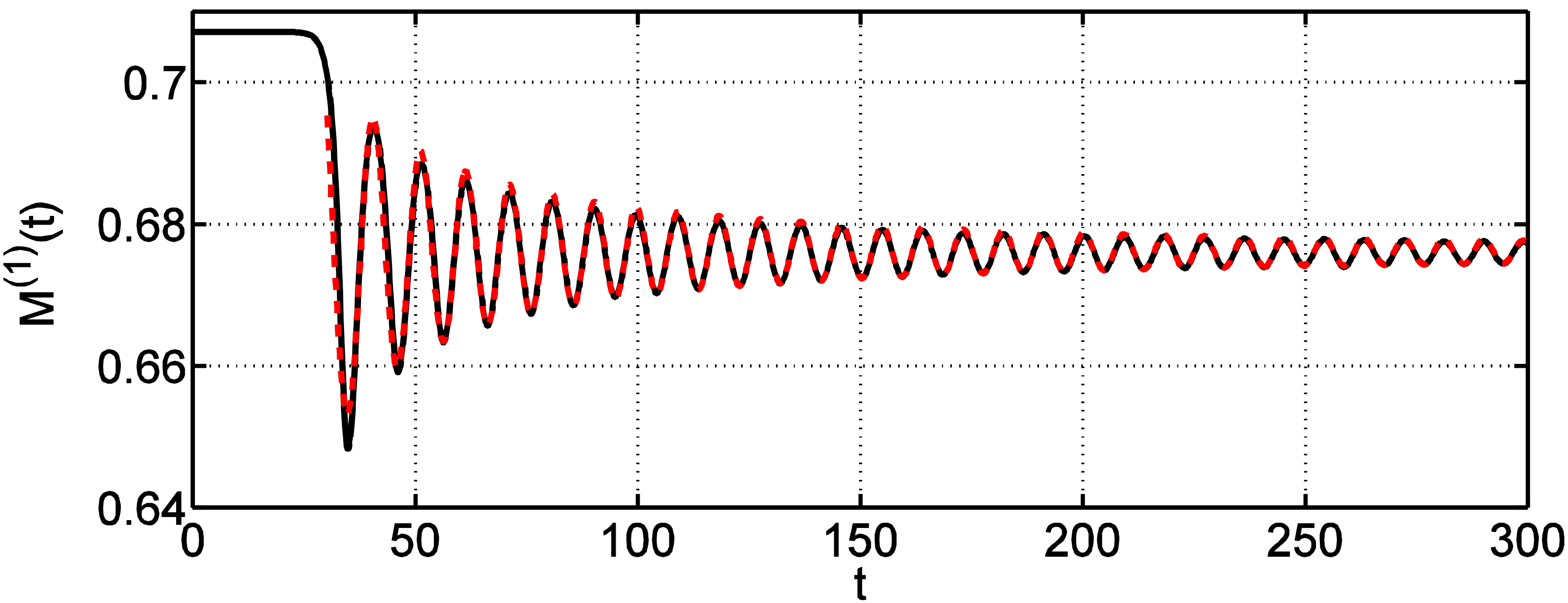

Oscillations of the moments are very well approximated by the model function,

$$M^{(n)}(t) \equiv \langle |\psi|^n \rangle \approx M_A^{(n)} + \frac{p}{t^\alpha}\sin(\Phi(t)), \quad \Phi(t) = st + \phi_{nl}(t) + \Phi_0, \quad \phi_{nl}(t) = \frac{q}{t^{1/2}}.$$

where $\mathbf{M_A^{(n)}}$ is asymptotic (non-Rayleigh!) value, **s** is the frequency, and ϕ_{nl} is the nonlinear phase shift.

Note, that in this case the exponent **1<α<1.5** varies for different moments and different cnoidal waves.

Numerical experiments with NLSE – cnoidal wave IC.

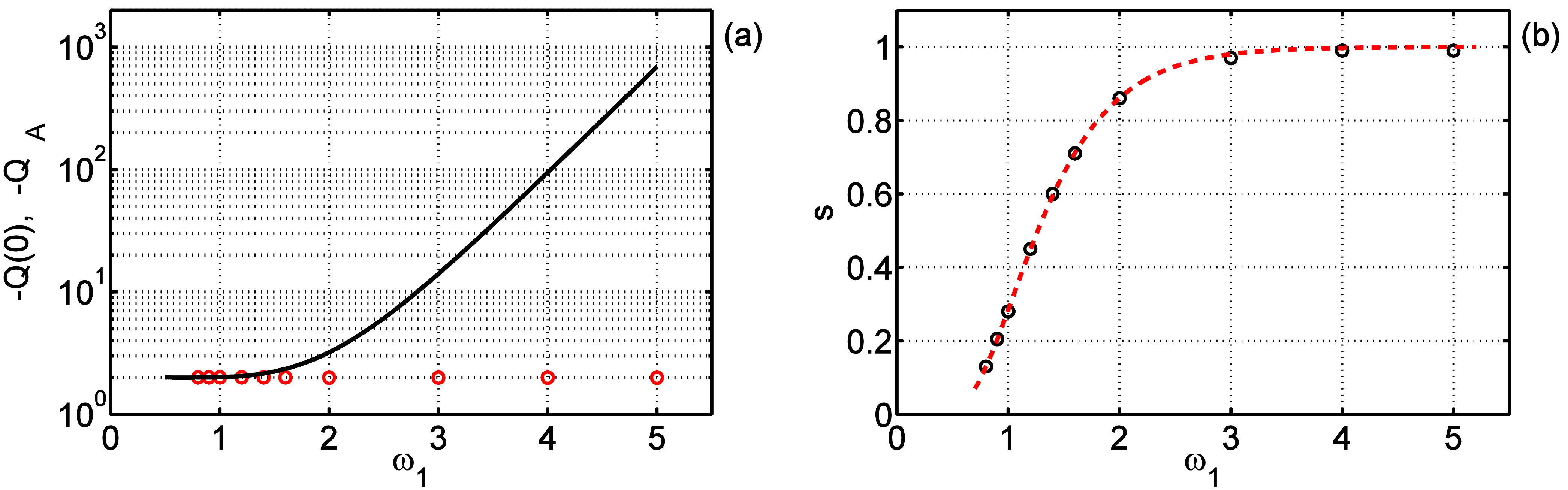

Left figure: in the asymptotic state, the potential to kinetic energy ratio is equal to 2, as for the condensate case. Here red circles are the final ratio, and black line is the initial one.

Right figure: the frequency of the oscillations **s** (black circles) is equal to the double maximal growth rate of the modulational instability (black dashed curve).

Numerical experiments with NLSE – cnoidal wave IC.

The PDF in the asymptotic state depends on the initial cnoidal wave. If the overlapping between solitons is small (left), when the PDF is significantly non-Rayleigh one. If the overlapping is large (right), then the PDF practically coincides with Rayleigh PDF.

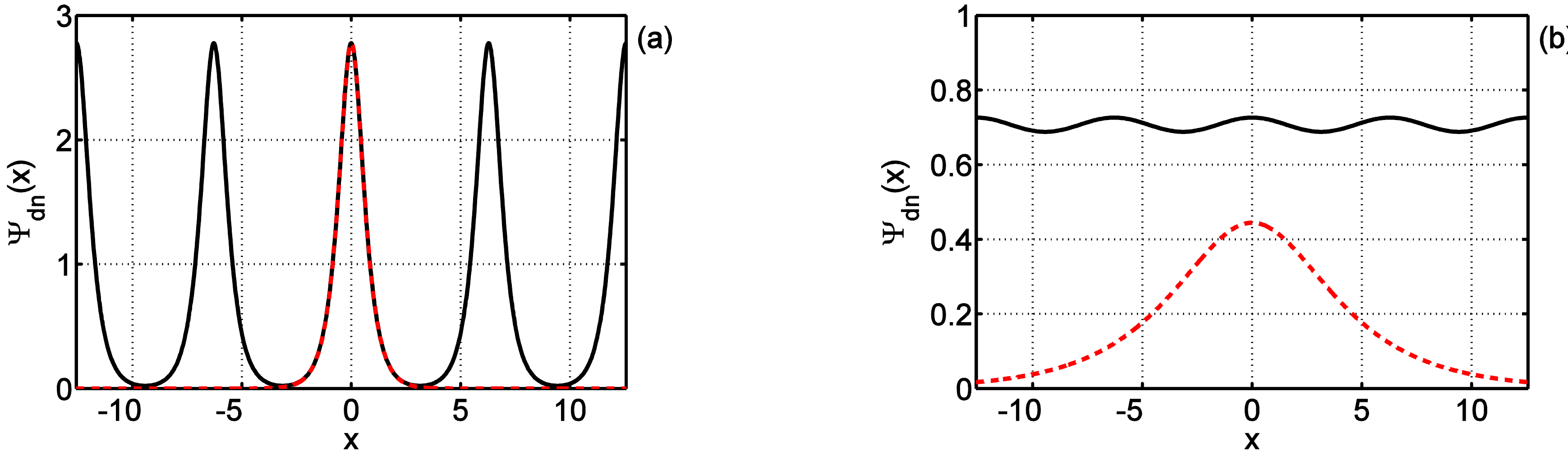

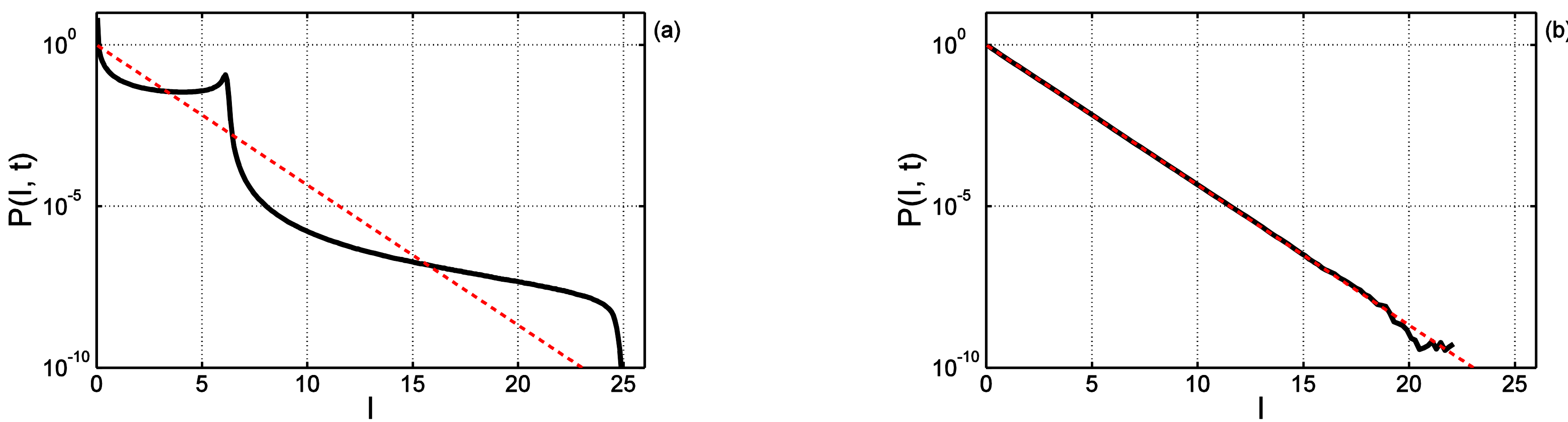

Numerical experiments with NLSE – Soliton gas IC.

$$\boldsymbol{\Phi}_0(\mathrm{x},\mathrm{t},\lambda) = \begin{pmatrix} e^{\phi_0(\mathrm{x},\mathrm{t},\lambda)} & 0 \\ 0 & e^{-\phi_0(\mathrm{x},\mathrm{t},\lambda)} \end{pmatrix}$$

$$\psi(x,t)_{NSS} = \psi(x,t)_{NSS-1} + 2i(\lambda_n - \lambda_n^*)\frac{q_{n,1}^* q_{n,2}}{(\boldsymbol{q_n}\cdot \boldsymbol{q_n^*})}$$

$$\boldsymbol{q_n} = \boldsymbol{\Phi}_{\boldsymbol{n-1}}^*(\mathrm{x},\mathrm{t},\lambda_n^*)\begin{pmatrix} c_n^{-1} \\ c_n \end{pmatrix} \qquad \boldsymbol{\Phi}_n(\mathrm{x},\mathrm{t},\lambda) = \boldsymbol{\chi}_n(\mathrm{x},\mathrm{t},\lambda)\cdot \boldsymbol{\Phi}_{n-1}(\mathrm{x},\mathrm{t},\lambda)$$

$$\chi_{n,\alpha\beta}(\lambda) = \delta_{\alpha\beta} + \frac{\lambda_n - \lambda_n^*}{\lambda - \lambda_n}\frac{q_{n,\alpha}^* q_{n,\beta}}{(\boldsymbol{q_n}\cdot \boldsymbol{q_n^*})}$$

Dressing method + high-precession arithmetic allows us to generate 128-soliton IC with high soliton spatial density

One-soliton solution (1-SS) :

$$\psi_{1SS}(x,t) = 2\beta\frac{\exp[-2i\alpha(x-x_0) - 2i(\alpha^2-\beta^2)t + i\theta]}{ch[2\beta(x-x_0) + 4\alpha\beta t]}$$

Scheme of the numerical experiment:

1. We generate 128-soliton solution with tails decaying at the ends of the numerical tank.

2. We run time evolution (numerically) and wait for stohastization (periodization) in soliton gas

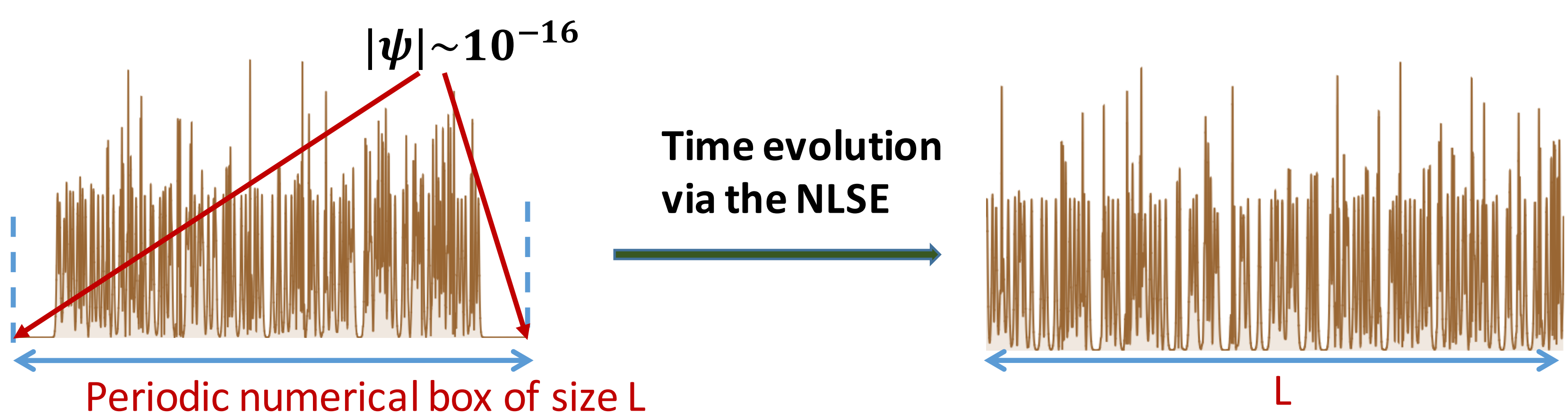

We study $10^3 \div 10^4$ statistical realizations of IC.
How we distribute soliton parameters?

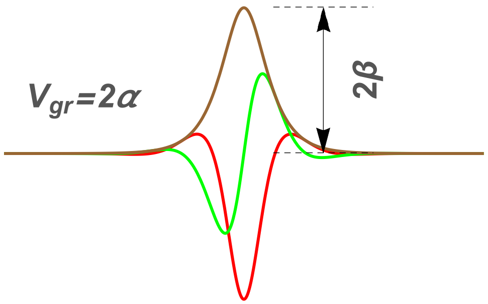

soliton phases $\theta_k \in$ random uniform distribution($[0, 2\pi]$),

soliton positions $x_{0k} \in$ random uniform distribution($[-\tilde{L}/2, \tilde{L}/2]$), $\tilde{L} < L$ (so that IC localized in L).

soliton eigenvalues $\lambda_k = \alpha_k + i\beta_k$ distribution:

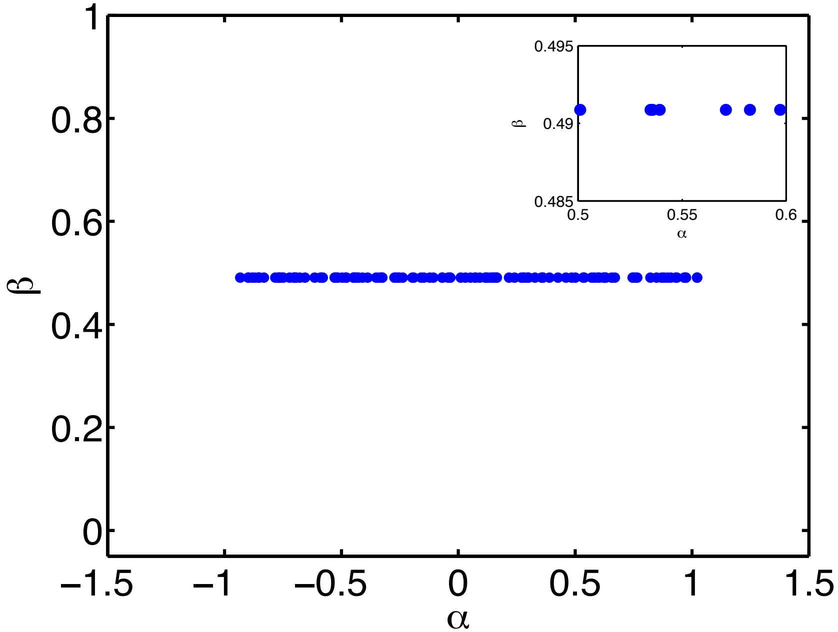

We choose all soliton amplitudes are equal:

$$\beta_k = \beta = \frac{\pi}{4 \cdot 1.6}, \qquad A_k = A = \frac{\pi}{2 \cdot 1.6} \approx 0.98.$$

All velocities are different, distributed uniformly in the interval:
$\alpha_k =$ uniform distribution$([-\sigma, \sigma])$

$$\cancel{\boldsymbol{\lambda_k = \lambda_j}}$$

We skip the degenerate case!

We introduce the eigenvalue small "guard interval", i.e. in our simulations:

$$\boldsymbol{\Delta\lambda}: \ |\boldsymbol{\lambda_k - \lambda_j}| > \boldsymbol{\Delta\lambda}, \qquad \forall \boldsymbol{k, j}$$

$\boldsymbol{\Delta\lambda \sim 10^{-9}}$ So that the influence of this restriction on statistics can be neglected

Example of 128-soliton solution calculated by the dressing method using high-precession arithmetic

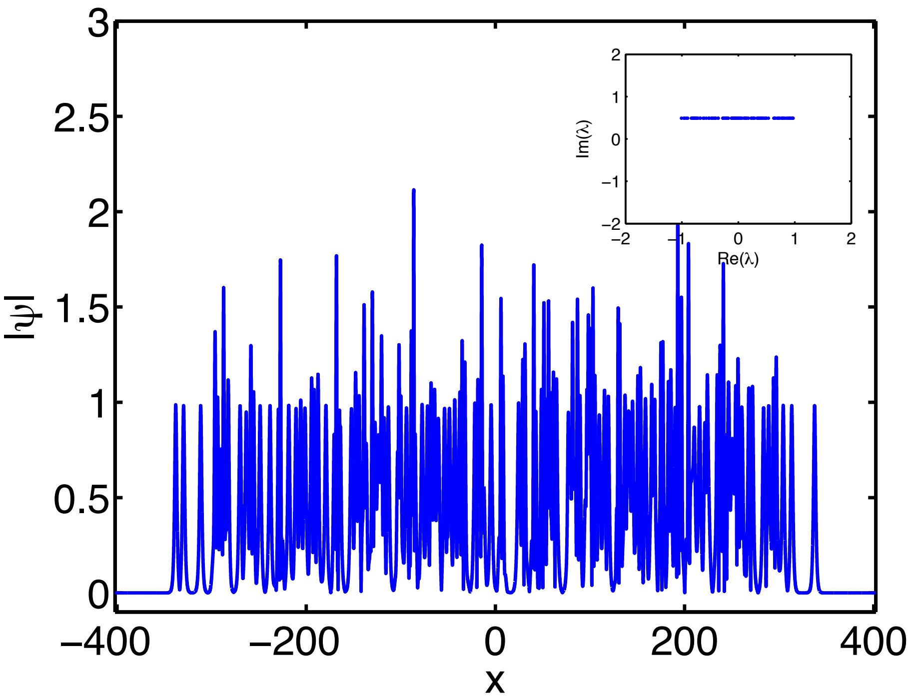

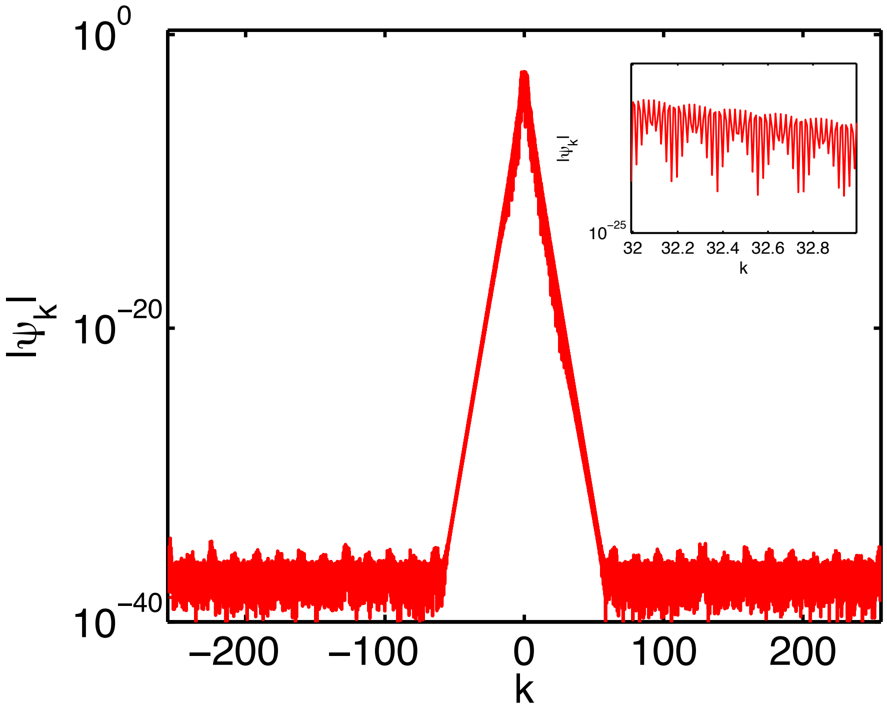

Absolute value of 128-soliton solution
On the inset picture we plot distribution of soliton eigenvalues

Fourier spectrum

We control, that during soliton gas stohastization (periodization), all statistical characteristics of the system become stationary:

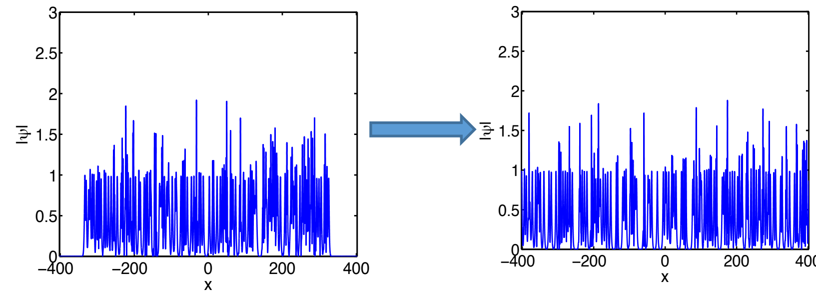

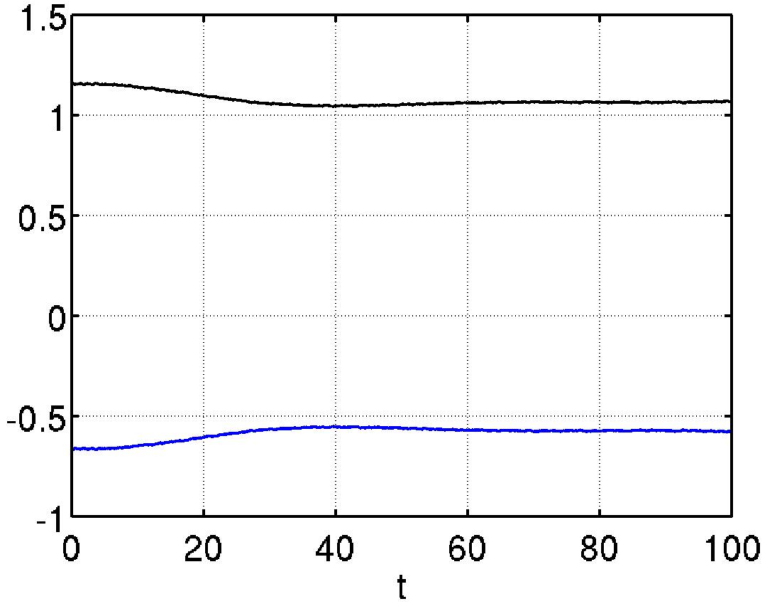

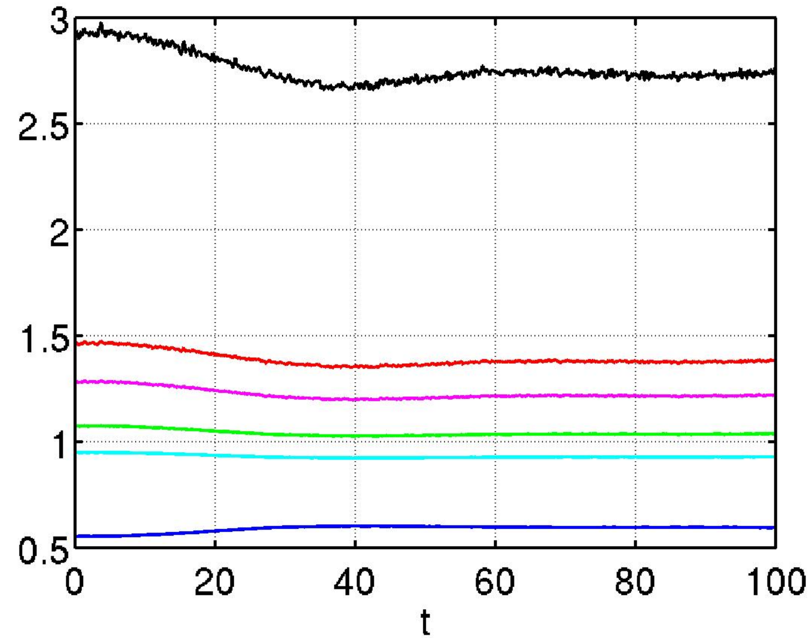

Kinetic energy $\boldsymbol{H_2 = \frac{1}{L}\int_{-L/2}^{L/2} |\psi_x|^2\, dx}$ (black curve)

and potential energy $\boldsymbol{H_4 = -\frac{1}{2L}\int_{-L/2}^{L/2} |\psi|^4 dx}$ (blue curve)

Statistical moments (first 5)

The complete stochastization of the solitonic ensemble occurs in a short period of time, since solitons in the dense gas frequently collide with each other acquiring additional phase-spatial shifts. After that we study statistical properties of our system.

The behaviour of soliton gas at different soliton densities

We found, that at high soliton densities, the PDF becomes Rayleigh distributed.

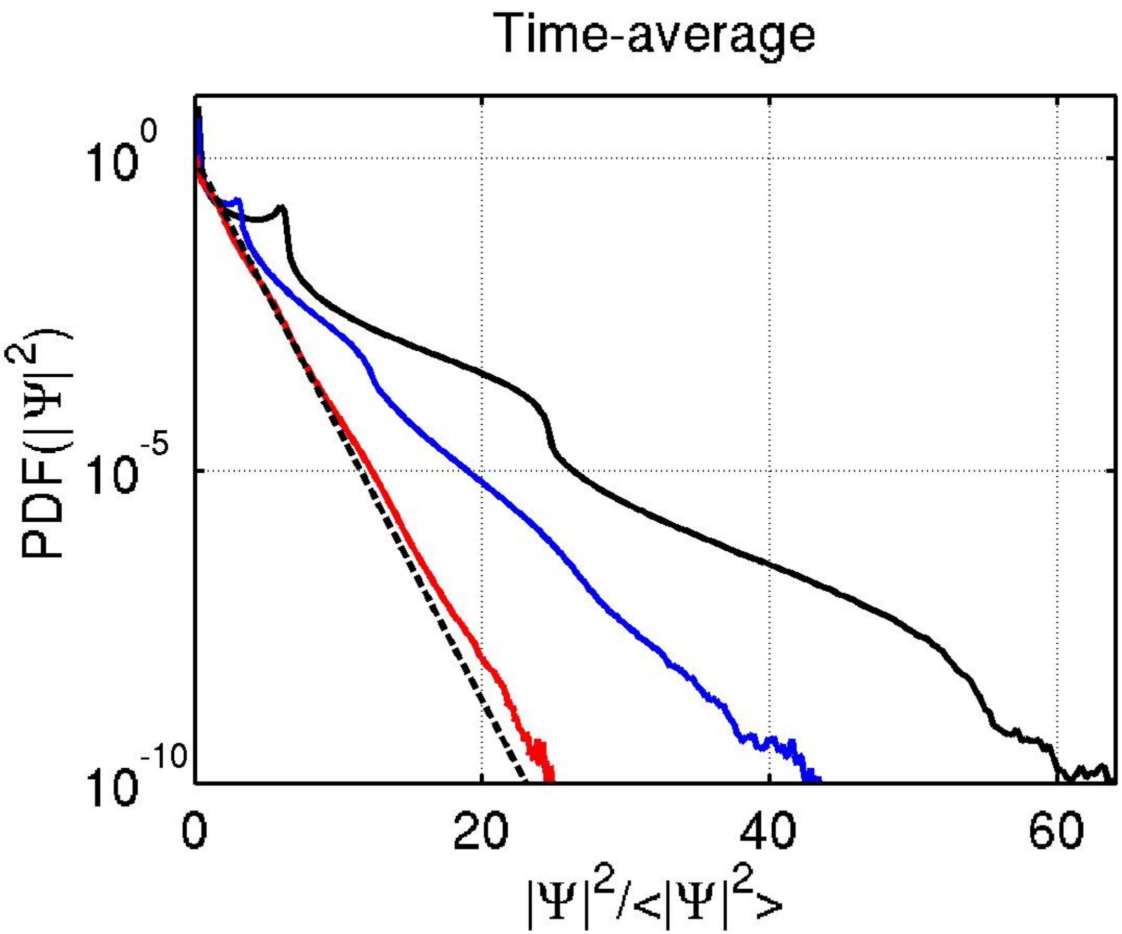

Probability Density Function for $|\psi|^2$

Black curve – low soliton spatial density, 128 solitons on the interval L = 256 π;

Blue curve – intermediate soliton spatial density, 128 solitons on L = 192 π

Red curve – high soliton spatial density, 128 solitons on L=128 π.

Black dotted line - Rayleigh distribution.

Numerical experiments with NLSE – references.

[1] D.S. Agafontsev, V.E. Zakharov, *Integrable turbulence and formation of rogue waves*, Nonlinearity 28, pp. 2791-2821 (2015).

[2] D.S. Agafontsev, V.E. Zakharov, *Integrable turbulence generated from modulational instability of cnoidal waves,* Nonlinearity 29, 3551-3578 (2016).

[3] A.A. Gelash, D.S. Agafontsev, *Statistic of dense soliton gas and formation of rogue waves*, In Preparation.

For generalized NLS equation, see also:

[4] D.S. Agafontsev, V.E. Zakharov, Intermittency in generalized NLS equation with focusing six-wave interactions, Phys. Lett. A 379, 2586-2590 (2015).